

4-Tap Wavelet Filters Using Algebraic Integers

Sravya.K¹, V.Santhosh Kumar²

¹PG Student, Electronics & Communication Engineering, Anurag Engineering College, Kodad, T.S, India

²Assistant Professor, Electronics & Communication Engineering, Anurag Engineering College, Kodad, T.S, India

Abstract: An Image is often corrupted by noise in its acquisition or transmission. The goal of denoising is to remove the noise while retaining as much as possible the important signal features. Traditionally, this is achieved by linear processing such as Wiener filtering. A vast literature has emerged recently on signal denoising using nonlinear techniques, in the setting of additive white Gaussian noise. The seminal work on signal denoising via wavelet thresholding have shown that various wavelet thresholding schemes for denoising have near-optimal properties in the minimax sense and perform well in simulation studies of one-dimensional curve estimation. It has been shown to have better rates of convergence than linear methods for approximating functions. Thresholding is a nonlinear technique, yet it is very simple because it operates on one wavelet coefficient at a time. Alternative approaches to nonlinear wavelet-based denoising can be found in, for example and references therein.

Keywords— Wavelet, Filter, 4 tap

I. INTRODUCTION

The field of discrete wavelet transforms (DWT) has been attracting substantial interest in part due to the wavelet analysis being capable of decomposing a signal into a particular set of basic functions equipped with good spectral properties. Wavelet analysis has been used to detect system nonlinearities by making use of its localization feature. DWTbased multi-resolution analysis leads to both time and frequency localization. Moreover, the proposed architecture is sought to be multiplier free. Such design facilitate accuracy, speed, relatively smaller area on chip as well as cost of design. The new design is multien-coded and multi-rate, operating over AI with no intermediate reconstruction steps. In this framework, error-free computations can be performed until the final FRS. Our architecture emphasizes on quality of output image and speed by trading complexity and power consumption for accuracy.

The intuition behind using lossy compression for denoising may be explained as follows. A signal typically has structural correlations that a good coder can exploit to yield a concise representation. White noise, however, does not have structural redundancies and thus is not easily compressible. Hence, a good compression method can provide a suitable model for distinguishing between signal and noise. The discussion will be restricted to wavelet-based coders, though these insights can be extended to other transform-domain coders as well. A concrete

connection between lossy compression and denoising can easily be seen when one examines the similarity between thresholding and quantization, the latter of which is a necessary step in a practical lossy coder. That is, the quantization of wavelet coefficients with a zero-zone is an approximation to the thresholding function. Thus, provided that the quantization outside of the zero-zone does not introduce significant distortion, it follows that wavelet-based lossy compression achieves denoising. With this connection in mind, this paper is about wavelet thresholding for image denoising and also for lossy compression. The threshold choice aids the lossy coder to choose its zero-zone, and the resulting coder achieves simultaneous denoising and compression if such property is desired.

Denoising i.e. restoration of electronically distorted images is an old but also still a relevant problem. There are many different cases of distortions. One of the most prevalent cases is distortion due to additive white Gaussian noise which can be caused by poor image acquisition or by transferring the image data in noisy communication channels. Early methods to restore the image used linear filtering or smoothing methods. These methods where simple and easy to apply but their effectiveness is limited since this often leads to blurred or smoothed out in high frequency regions. All denoising methods use images artificially distorted with well defined white Gaussian noise to achieve objective test results. Note however that in real world images, to discriminate the distorting signal from the “true” image is an ill posed problem since it is not always well defined whether a pixel value belongs to the image or it is part of unwanted noise. Newer and better approaches perform some thresholding in the wavelet domain of an image. The idea of wavelet thresholding relies on the assumption that the signal magnitudes dominate the magnitudes of the noise in a wavelet representation, so that wavelet coefficients can be set to zero if their magnitudes are less than a predetermined threshold. More recent developments focus on more sophisticated methods, like local or context-based thresholding in the wavelet domain. Some methods are inspired by wavelet-based image compression methods.

The theoretical formalization of filtering additive iid Gaussian noise (of zero-mean and standard deviation) via thresholding wavelet coefficients was pioneered by Donoho and Johnstone. A wavelet coefficient is compared to a given threshold and is set to zero if its magnitude is less than the threshold; otherwise, it is

kept or modified (depending on the thresholding rule). The threshold acts as an oracle which distinguishes between the insignificant coefficients likely due to noise, and the significant coefficients consisting of important signal structures. Thresholding rules are especially effective for signals with sparse or near-sparse representations where only a small subset of the coefficients represents all or most of the signal energy. Thresholding essentially creates a region around zero where the coefficients are considered negligible. Outside of this region, the thresholded coefficients are kept to full precision (that is, without quantization).

Since the works of Donoho and Johnstone, there has been much research on finding thresholds for nonparametric estimation in statistics. However, few are specifically tailored for images. In this project, we propose a framework and a near-optimal threshold in this framework more suitable for image denoising. This approach can be formally described as Bayesian, but this only describes our mathematical formulation, not our philosophy. The formulation is grounded on the empirical observation that the wavelet coefficients in a sub band of a natural image can be summarized adequately by a *generalized Gaussian distribution* (GGD). This observation is well-accepted in the image processing community and is used for state-of-the-art image coders. It follows from this observation that the average MSE (in a sub band) can be approximated by the corresponding Bayesian squared error risk with the GGD as the prior applied to each in an *iid* fashion. That is, a sum is approximated by an integral. We emphasize that this is an analytical approximation and our framework is broader than assuming wavelet coefficients are *iid* draws from a GGD. The goal is to find the soft-threshold that minimizes this Bayesian risk, and we call our method *BayesShrink*.

The GGD, following is

$$GG_{\sigma_X, \beta}(x) = C(\sigma_X, \beta) \exp\{-[\alpha(\sigma_X, \beta)|x|]^\beta\}$$

$-\infty < x < \infty, \sigma_X > 0, \beta > 0$, where

$$\alpha(\sigma_X, \beta) = \sigma_X^{-1} \left[\frac{\Gamma(3/\beta)}{\Gamma(1/\beta)} \right]^{1/2}$$

and

$$C(\sigma_X, \beta) = \frac{\beta \cdot \alpha(\sigma_X, \beta)}{2\Gamma\left(\frac{1}{\beta}\right)}$$

Adaptive wavelet thresholding for image denoising and compression is shown in fig 1.

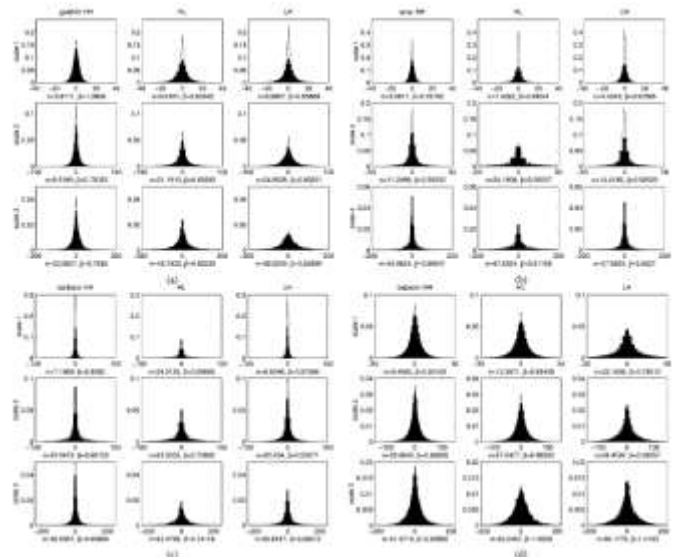
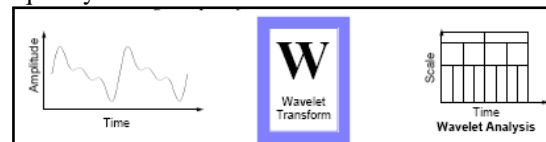


Figure 1: Histogram of the wavelet coefficients of four test images

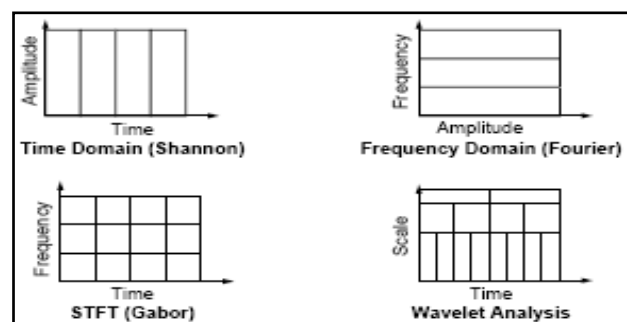
For each image, from top to bottom it is fine to coarse scales: from left to right, they are the HH, HL, and LH sub bands, respectively.

II. WAVELET ANALYSIS

Wavelet analysis represents the next logical step: a windowing technique with variable-sized regions. Wavelet analysis allows the use of long time intervals where we want more precise low-frequency information, and shorter regions where we want high-frequency information.



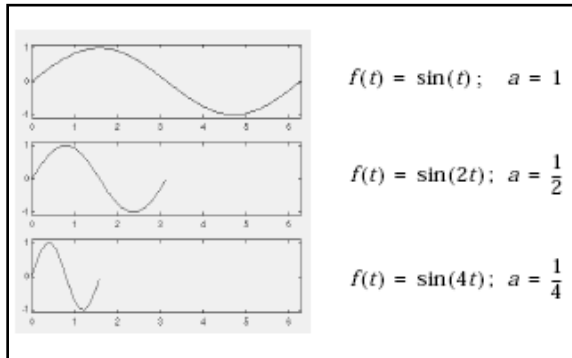
Here's what this looks like in contrast with the time-based, frequency-based, and STFT views of a signal:



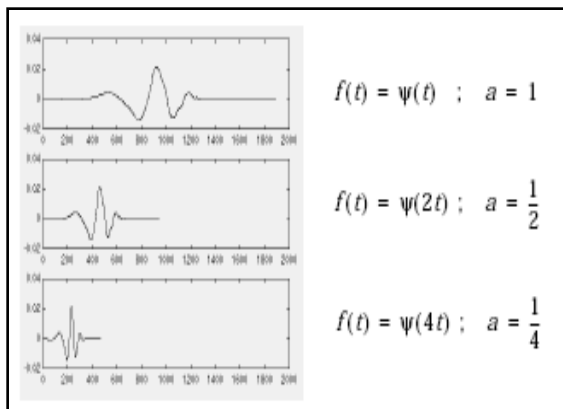
You may have noticed that wavelet analysis does not use a time-frequency region, but rather a time-scale region. For more information about the concept of scale and the link between scale and frequency, see "How to Connect Scale to Frequency?"

We've already alluded to the fact that wavelet analysis produces a time-scale view of a signal and now we're talking about scaling and shifting wavelets. What

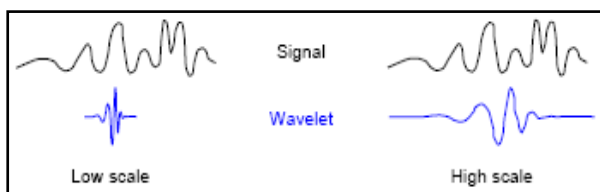
exactly do we mean by *scale* in this context? Scaling a wavelet simply means stretching (or compressing) it. To go beyond colloquial descriptions such as “stretching,” we introduce the scale factor, often denoted by the letter *a*. If we’re talking about sinusoids, for example the effect of the scale factor is very easy to see:



The scale factor works exactly the same with wavelets. The smaller the scale factor, the more “compressed” the wavelet.



It is clear from the diagrams that for a sinusoid $\sin(\omega t)$ the scale factor ‘*a*’ is related (inversely) to the radian frequency ‘ ω ’. Similarly, with wavelet analysis the scale is related to the frequency of the signal. Notice that the scales in the coefficients plot (shown as y-axis labels) run from 1 to 31. Recall that the higher scales correspond to the most “stretched” wavelets. The more stretched the wavelet, the longer the portion of the signal with which it is being compared, and thus the coarser the signal features being measured by the wavelet coefficients.



Thus, there is a correspondence between wavelet scales and frequency as revealed by wavelet analysis:

- Low scale $a \Rightarrow$ Compressed wavelet \Rightarrow rapidly changing details \Rightarrow High frequency ‘ ω ’.
- High scale $a \Rightarrow$ Stretched wavelet \Rightarrow slowly changing, coarse features \Rightarrow Low frequency ‘ ω ’.

III. AI-BASED DAUBECHIES-4 AND -6 SCALING FILTERS

An algebraic integer is a real or complex number that is a root of a monic polynomial with integer coefficients. Algebraic integers can be employed to define encoding mappings which can precisely represent particular irrational numbers by means of usual integers. Considering the roots of the monic polynomials $x^2 - 3$, $x^2 - 10$, and $x^4 - 10x^2 - 15 = 0$ we can extend the set of integers by including the algebraic integer $\zeta = \sqrt{3}$, $\zeta_1 = \sqrt{10}$ and $\zeta_2 = \sqrt{5 + 2\sqrt{10}}$. Doing so, a given quantity can possibly be represented as

$$y = a + b \cdot \zeta$$

$$y = c + d \cdot \zeta_1 + e \cdot \zeta_2 + f \cdot \zeta_1 \zeta_2.$$

where a, b, c, d, e and f are integers. Sets $(1, \text{dash})$ and $\{1, \zeta_1, \zeta_2, \zeta_1 \zeta_2\}$ constitute two bases for AI encoding. Notice that these two bases are adequate for representing the 4- and 6-tap Daubechies filter coefficients. Thus, taking apart quantities $1/\beta_1 = 4\sqrt{2}$ and $1/\beta_2 = 16\sqrt{2}$ as scaling factors, the Daub-4 and -6 filter coefficients can be represented as

$$\mathbf{h}^{(\text{Daub-4})} = [1 + \zeta \quad 3 + \zeta \quad 3 - \zeta \quad 1 - \zeta]^T$$

$$\mathbf{h}^{(\text{Daub-6})} = \begin{bmatrix} 1 + \zeta_1 + \zeta_2 \\ 5 + \zeta_1 + 3\zeta_2 \\ 10 - 2\zeta_1 + 2\zeta_2 \\ 10 - 2\zeta_1 - 2\zeta_2 \\ 5 + \zeta_1 - 3\zeta_2 \\ 1 + \zeta_1 - \zeta_2 \end{bmatrix}.$$

Therefore, these un normalized low-pass FIR filters of 4-tap/6-tap can be split into separate filters given by

$$\mathbf{h}^{(\text{Daub-4})} = \mathbf{h}_1 + \zeta \cdot \mathbf{h}_\zeta$$

$$\mathbf{h}^{(\text{Daub-6})} = \mathbf{h}'_1 + \zeta_1 \cdot \mathbf{h}_{\zeta_1} + \zeta_2 \cdot \mathbf{h}_{\zeta_2}$$

Where,

$$\begin{aligned} \mathbf{h}_1 &= [1 \ 3 \ 3 \ 1]^T \\ \mathbf{h}_\zeta &= [1 \ 1 \ -1 \ -1]^T \\ \mathbf{h}'_1 &= [1 \ 5 \ 10 \ 10 \ 5 \ 1]^T \\ \mathbf{h}_{\zeta_1} &= [1 \ 1 \ -2 \ -2 \ 1 \ 1]^T \\ \mathbf{h}_{\zeta_2} &= [1 \ 3 \ 2 \ -2 \ -3 \ -1]^T. \end{aligned}$$

Level	Base	Expression
1	$A_1^{(1)}$	$h_1 \oplus h_1 \oplus A_1 \oplus 3 \cdot h_1 \oplus h_1 \oplus A_1$
	$A_1^{(2)}$	$h_\zeta \oplus h_\zeta \oplus A_1 \oplus h_1 \oplus h_1 \oplus A_1$
2	$A_2^{(1)}$	$h_1 \oplus h_1 \oplus A_1^{(1)} \oplus 3 \cdot h_1 \oplus h_1 \oplus A_1^{(1)} \oplus h_1 \oplus h_1 \oplus A_1^{(1)} \oplus h_1 \oplus h_1 \oplus A_1^{(1)}$
	$A_2^{(2)}$	$h_\zeta \oplus h_\zeta \oplus A_1^{(2)} \oplus 3 \cdot h_\zeta \oplus h_\zeta \oplus A_1^{(2)} \oplus h_\zeta \oplus h_\zeta \oplus A_1^{(2)} \oplus h_\zeta \oplus h_\zeta \oplus A_1^{(2)}$
n	$A_n^{(1)}$	$h_1 \oplus h_1 \oplus A_{n-1}^{(1)} \oplus 3 \cdot h_1 \oplus h_1 \oplus A_{n-1}^{(1)} \oplus 3 \cdot h_1 \oplus h_1 \oplus A_{n-1}^{(1)} \oplus 3 \cdot h_1 \oplus h_1 \oplus A_{n-1}^{(1)}$
	$A_n^{(2)}$	$h_\zeta \oplus h_\zeta \oplus A_{n-1}^{(2)} \oplus 3 \cdot h_\zeta \oplus h_\zeta \oplus A_{n-1}^{(2)} \oplus h_\zeta \oplus h_\zeta \oplus A_{n-1}^{(2)} \oplus h_\zeta \oplus h_\zeta \oplus A_{n-1}^{(2)}$

DAUB-4 DECOMPOSITIONS:

Therefore, the Daub-4 and -6 filter bank analysis can be separated into two/three structures. This facilitates a two/four integer channel structure, where the integer coefficient filters h_ζ ; and h'_1, h_{ζ_1} and h_{ζ_2} and are considered. All implied computations are necessarily over an integer field. Notice that a usual integer can be effortlessly represented in either basis:

$$\begin{aligned} m &= m + 0 \cdot \zeta \\ m &= m + 0 \cdot \zeta_1 + 0 \cdot \zeta_2 + 0 \cdot \zeta_1 \zeta_2. \end{aligned}$$

This is relevant for encoding image pixel values, which are integers. In practical terms, this means that no circuitry for encoding integer input data is necessary. AI based Daub-4 and -6 filter structures are shown in Fig. 2. These filters possess zero initial condition

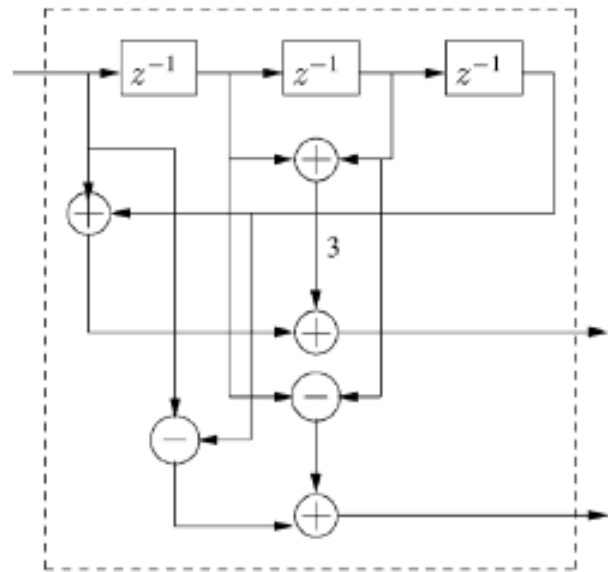


Figure 2: Daub-4 AI Filter Structure

2-D Filtering:

We now provide the mathematical framework to describe the operation of the proposed AI-based multi-level encoding design. The following notation is adopted in this work. Let C be an Nby N matrix with columns $c_j, j=0,1,\dots,N-1$ $C=[c_0 \ c_1 \ c_2 \dots \ c_{N-1}]$ and be an -point column vector. The operation \boxtimes is defined according to

$$\begin{aligned} \mathbf{v} \boxtimes \mathbf{C} &\triangleq (2 \downarrow 1) [\mathbf{v} * \mathbf{c}_0 \ \mathbf{v} * \mathbf{c}_1 \ \mathbf{v} * \mathbf{c}_2 \ \dots \ \mathbf{v} * \mathbf{c}_{N-1}] \\ &= [\mathbf{v} * \mathbf{c}_0 \ \mathbf{v} * \mathbf{c}_2 \ \dots \ \mathbf{v} * \mathbf{c}_{N-2}], \end{aligned}$$

Where $*$ is the convolution operation? Analogously, operation is given by:

$$\mathbf{v} \ominus \mathbf{C} \triangleq (\mathbf{v} \boxtimes \mathbf{C}^T)^T$$

In other words \boxtimes and \ominus are the filtering operations along the rows and columns of a given image, respectively, followed by a dyadic down-sampling stage.

IV. RESULTS

The results indicates the image input pixels are stored in the memory .the pixels in hexadecimal are shown in image_reg storage.



the result above indicates the image input pixels are stored in the memory .the pixels in hexadecimal are shown in image_reg storage.



the above simulation shows the pixels values selected in a colour wise format images.

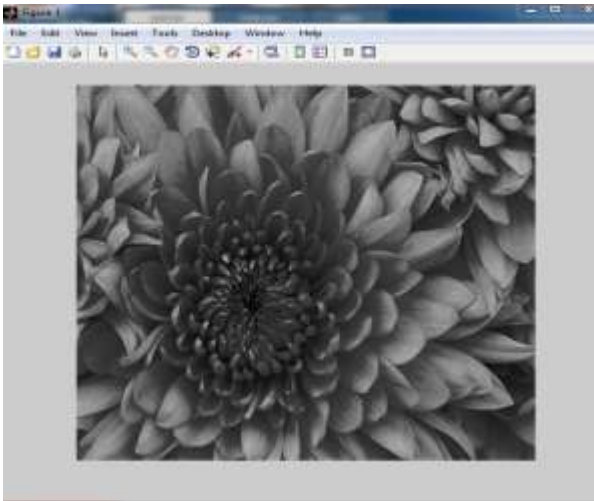


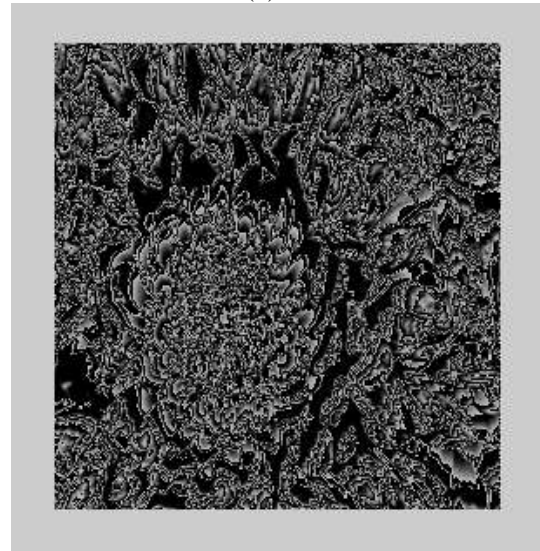
Figure 3: input image



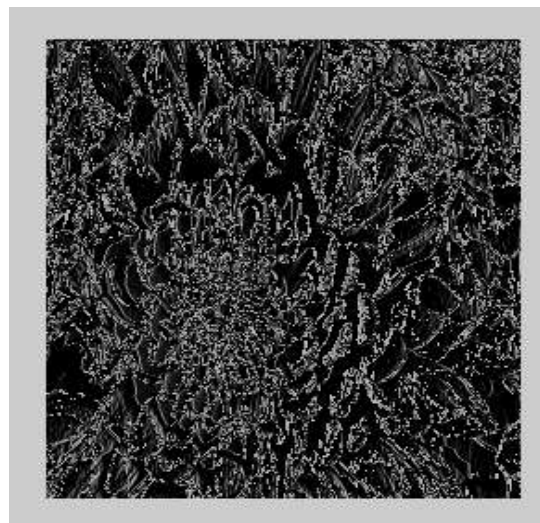
(a)



(b)



(c)



(d)

Figure 4: Decomposition of dwt levels

V. CONCLUSION

In this project 4 tap and 6 tap dwt is done for computing DWT/IDWT. Using this architecture proposed in this project Windowing technique of the paper is to provide zoom in and zooms out of image. Here, coefficients are used as a tool to increase/decrease image size, even though image is not of size $2^n \times 2^n$ where n is an integer. Zero padding technique is used for images those are not of size $2^n \times 2^n$ dimensions. The main advantage of the proposed architecture is its inherent speed due to elimination of the multipliers in computing DWT/IDWT. The algebraic integers Algorithm is used for computing DWT/IDWT. The proposed architecture provides flexibility to implementing and provides zoom in and zooms out of images of various sizes. Scope for further work is by slight modification of the architecture we can achieve reduction in size until it reaches two pixels.

References

1. K. A. Wahid, V. S. Dimitrov, and G. A. Jullien, "Error-free arithmetic for discrete wavelet transforms using algebraic integers," in *Proc. 16th IEEE Symp. Computer Arithmetic*, 2003, pp. 238–244.
2. S.-C. B. Lo, H. Li, and M. T. Freedman, "Optimization of wavelet decomposition for image compression and feature preservation," *IEEE Trans. Med. Imag.*, vol. 22, no. 9, pp. 1141–1151, Sep. 2003.
3. M. Martone, "Multiresolution sequence detection in rapidly fading channels based on focused wavelet decompositions," *IEEE Trans. Commun.*, vol. 49, no. 8, pp. 1388–1401, 2001.
4. P. P. Vaidyanathan, *Multirate Systems and Filter Banks*. Englewood Cliffs, NJ: PTR Prentice Hall, 1992, 07632.
5. D. B. H. Tay, "Balanced spatial and frequency localised 2-D nonseparable wavelet filters," in *Proc. IEEE Int. Symp. Circuits Systems ISCAS 2001*, 2001, vol. 2, pp. 489–492.
6. M. A. Islam and K. A. Wahid, "Area- and power-efficient design of Daubechies wavelet transforms using folded AIQ mapping," *IEEE Trans. Circuits Syst. II, Exp. Briefs*, vol. 57, no. 9, pp. 716–720, Sep. 2010.
7. F. Marino, D. Guevorkian, and J. T. Astola, "Highly efficient high-speed/low-power architectures for the 1-D discrete wavelet transform," *IEEE Trans. Circuits Syst. II, Exp. Briefs*, vol. 47, no. 12, pp. 1492–1502, Dec. 2000.
8. K. A. Wahid, V. S. Dimitrov, G. A. Jullien, and W. Badawy, "Error-free computation of Daubechies wavelets for image compression applications," *Electron. Lett.*, vol. 39, no. 5, pp. 428–429, 2003.
9. T. Acharya and P.-Y. Chen, "Vlsi implementation of a dwt architecture," in *Proc. IEEE Int. Symp. Circuits Syst. ISCAS'98*, 1998, vol. 2, pp. 272–275.
10. S. Gnani, B. Penna, M. Grangetto, E. Magli, and G. Olmo, "DSP performance comparison between lifting and filter banks for image coding," in *Proc. IEEE Int. Acoustics, Speech, Signal Processing (ICASSP) Conf.*, 2002, vol. 3.
11. A. M. M. Maamoun, M. Neggazi, and D. Berkani, "VLSI design of 2-D discrete wavelet transform for area efficient and high-speed image computing," *World Acad. Science, Eng. Technol.*, vol. 45, pp. 538–543, 2008.
12. I. Urriza, J. I. Artigas, J. I. Garcia, L. A. Barragan, and D. Navarro, "VLSI architecture for lossless compression of medical images using the discrete wavelet transform," in *Proc. Design, Automat. Test Eur.*, 1998, pp. 196–201.
13. R. Baghaie and V. Dimitrov, "Computing Haar transform using algebraic integers," in *Proc. Conf. Signals, Systems Computers Record 34th Asilomar Conf.*, 2000, vol. 1, pp. 438–442.
14. K. A. Wahid, M. A. Islam, and S.-B. Ko, "Lossless implementation of Daubechies 8-tap wavelet transform," in *Proc. IEEE Int. Symp. Circ. Syst.*, Rio de Janeiro, Brazil, May 2011, pp. 2157–2160.

Author's Profile

- K.SRAVYA is a PG student pursuing her M.Tech in VLSI & SD specialization in Anurag Engineering College, Kodad.
- V.SANTHOSH KUMAR is working as Assistant Professor in the department of ECE in Anurag Engineering College, Kodad. He has 3 years of teaching experience. He has published several papers on his research work.